

Kinematic analysis and design of a new two-limb parallel Schönflies-motion generator considering isotropic configuration

Guanglei Wu¹, Huiping Shen²

¹School of Mechanical Engineering, Dalian University of Technology, Dalian, China

²School of Mechanical Engineering, Changzhou University, Jiangsu, China

Article Info

Article history:

Received Feb 10, 2021

Revised May 25, 2021

Accepted Jun 23, 2021

Keywords:

Kinematic isotropy

Parallel robot

Schönflies-motion generator

Singularity

ABSTRACT

This paper presents a new two-limb parallel Schönflies-motion generator, which adopts a pair of alternative spatial modules equivalent to the parallelogram structure. This modular architecture can ensure the enhanced stiffness of the manipulator normal to the motion of the planar parallelogram structure due to the trapezoidal architecture. The preliminary kinematic problems, namely, the mobility, forward/inverse geometry and singularity, are studied as well as the kinematic isotropy. A neutral isotropic configuration of the robot is identified for the structural design of the link lengths.

This is an open access article under the [CC BY-SA](https://creativecommons.org/licenses/by-sa/4.0/) license.



Corresponding Author:

Guanglei Wu

School of Mechanical Engineering, Dalian University of Technology

116024 Dalian, Liaoning, China

Email: gwu@dlut.edu.cn

1. INTRODUCTION

Parallel robots with Schönflies-motion (three independent translations and one rotation around a fixed axis), also known as, selective compliance assembly robot arm (SCARA) motion [1], named as parallel Schönflies-motion generators, are more and more attractive for high-speed pick-and-place (PnP) applications serving light industries, thanks to their lightweight architecture and high stiffness. Amongst this type of robots [2]-[8], most of them so far have the symmetric structure with four identical limbs, which admit a cylindrical workspace. On the other hand, the PnP operations of the robots deployed in the production line are usually confined in a rectangular region. In view of the properties of PnP motion, the PnP robots with rectangular workspace are desired, allowing more robots to be installed side-by-side, to utilize the shop-floor space more efficiently. For this purpose, besides the recently developed asymmetrical four-limb robot [9], the architecture of the two-limb Schönflies-motion generators (SMGs) can effectively reduce the mounting space.

The design and development of the two-limb SMGs have been reported in the literature. For instance, Angeles *et al.* [10] developed the McGill SMG with two parallelogram structures (II joint) in one limb, which has a rectangular mounting space. On the other hand, the second floating motor in each limb leads to the increased inertia. Later, Lee and Lee [11] proposed several asymmetric SMGs with fewer links, which behaves isotropic kinematic and static performances. Harada and Angeles [12] selected one robot architecture from the previous work for prototyping, named as “Pepper Mill Carrier”. Although this robot architecture simplified the robot linkage design, the complexity of the actuation system increases due to the left/right-hand ball-screw driven structure. Some other designs inspired from this concept have also been reported [13], [14]. It should

be noted that this asymmetric architecture results in the property of unbalanced dynamics [15]. Another design of the five-bar based two-limb SMG [16] has fixed motor to reduce the inertia, but with decreased stiffness and limited motion along vertical axis. Linear actuated two-limb SMG developed by Wu *et al.* [17] can have almost the same workspace along its linear rail of the actuator. The previous two-limb SMGs saved shop-floor space due to their architecture, whereas, the stiffness along some motion axis decreased, unlike the fully symmetrical four-limb SMGs. Upon the investigation of the stiffness behavior [18], the stiffness along the normal to the motion of the planar parallelogram structure can be improved with an alternative spatial module, which can have different architectures [19], [20], towards high dynamic response. Table 1 lists a brief comparison of the reported two-limb SMGs. This paper will present the kinematic analysis of a new two-limb parallel Schönflies-motion generator based on the lightweight design of the pair of spatial modules.

In this paper, a new two-limb parallel Schönflies-motion generator is introduced, which adopts a pair of alternative spatial modules equivalent to the parallelogram structure. This modular architecture can ensure the enhanced stiffness of the manipulator normal to the motion of the planar parallelogram structure due to the trapezoidal architecture. The kinematic problems, namely, the mobility, forward/inverse geometry and singularity, are studied as well as the kinematic isotropy. A neutral isotropic configuration of the robot is identified for the structural design of the link lengths.

Table 1. Comparison of the reported two-limb SMGs

SMGs	Advantages	Disadvantages
McGill SMG [10]	Fewer links	Increased dynamic inertia due to movable motors
C-driven SMGs [12]-[14]	Fewer links, isotropic kinematic and static performances	Inherently unbalanced dynamics, complex cylindrical joint design
Five-bar based SMG [16]	Fewer links, low dynamic inertia	Decreased stiffness, limited motion along vertical axis
Linear SMG [17]	Large workspace along its linear rail of the actuator	Decreased stiffness along the linear rail
Proposed SMG	Enhanced stiffness, fewer linkages	Trapezoidal lower linkages, more kinematic joints

2. RESEARCH METHOD

2.1. Manipulator architecture

Figure 1 depicts the conceptual design of the two-limb parallel Schönflies-motion manipulator, for which each limb of the robot is actuated by two perpendicular actuators on the base. A pair of spatial modules, instead of the conventional Π joints, are adopted to connect the mobile platform and the proximal links.

The parameterized kinematic structure of the robot is illustrated in Figure 2, where the global coordinate frame \mathcal{F}_b is built with the origin located at the geometric center of the base platform, the x -axis being collinear to segment A_1A_2 . The moving coordinate frame \mathcal{F}_p is attached to the mobile platform and the origin is at the geometric center, where X -axis is parallel to segment C_1C_2 . Here and after, vectors \mathbf{i} , \mathbf{j} and \mathbf{k} represent the unit vectors of x -, y - and z -axis, respectively. The axis of rotation of the ij th actuated joint of angular displacement $\theta_{ij} \in (-\pi/2, \pi/2)$, $i = 1, 2$, $j = 1, 2$, is parallel to $\mathbf{u}_{ij} = \mathbf{R}(z, \alpha_{ij})\mathbf{j}$, $\alpha_{ij} = (-1)^{i+1}\pi/2 + (-1)^j\pi/4$. Moreover, as the offset distance e on the elbow bracket does not affect the output variable, but is added as an offset to z -coordinate, henceforth, the offset distance e is assumed to be zero for convenience.

2.2. Degree-of-freedom and displacement group

The degree-of-freedom (DOF) of the robot under study is derived by the group theory, consequently, according to Figure 3, the bond \mathcal{L}_i of the i th limb is the product of the following bonds i) The rotation subgroup $\mathcal{R}(\mathcal{A}_{ij})$ of axis of rotation \mathcal{A}_{ij} passing through A_{ij} and parallel to \mathbf{u}_{ij} ; ii) The translation subgroup $\mathcal{T}(\mathbf{n}_{ij})$ corresponding to the Π -joint lying in a plane ε_{ij} normal to \mathbf{n}_{ij} ; iii) The motion subgroup of the spatial module being the product of rotation subgroup $\mathcal{R}(\mathcal{B}_i)$ of axis of rotation \mathcal{B}_i passing through B_i and translation subgroup $\mathcal{T}(y)$ normal to y -axis; and iv) The rotation subgroup $\mathcal{R}(\mathcal{C}_i)$ axis of rotation \mathcal{C}_i passing through C_i and parallel to \mathbf{k} . Thus, the kinematic bonds of the i th limb is expressed as (1) and (2).

$$\begin{aligned}\mathcal{L}_i \& = (\mathcal{R}(\mathcal{A}_{i1}) \cdot \mathcal{T}(\mathbf{n}_{i1}) \cap \mathcal{R}(\mathcal{A}_{i2}) \cdot \mathcal{T}(\mathbf{n}_{i2})) \mathcal{R}(\mathcal{B}_i) \cdot \mathcal{T}(\mathbf{m}_i) \cdot \mathcal{R}(\mathcal{C}_i) \\ \& = \mathcal{T}(\mathbf{n}_i) \cdot \mathcal{R}(\mathcal{B}_i) \cdot \mathcal{T}(\mathbf{y}) \cdot \mathcal{R}(\mathcal{C}_i) = \mathcal{R}(\mathcal{B}_i) \cdot \mathcal{X}(\mathbf{k})\end{aligned}\quad (1)$$

Where \mathbf{n}_i is perpendicular to \mathbf{v}_i . Subsequently, the intersection of the bonds \mathcal{L}_1 and \mathcal{L}_2 yields.

$$\mathcal{L}_1 \cap \mathcal{L}_2 = \mathcal{X}(\mathbf{k}) \quad (2)$$

Henceforth, the intersection of all subgroups being a Schönflies subgroup $\mathcal{X}(\mathbf{k})$, the robot generates the Schönflies motion.

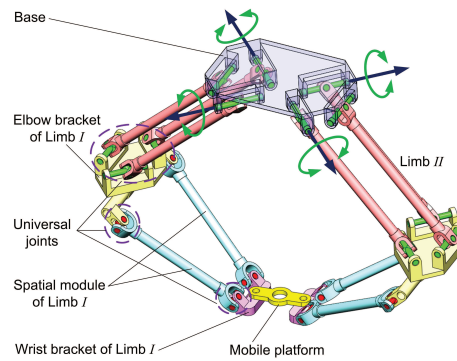


Figure 1. The conceptual design of the new two-limb parallel Schönflies-motion robot

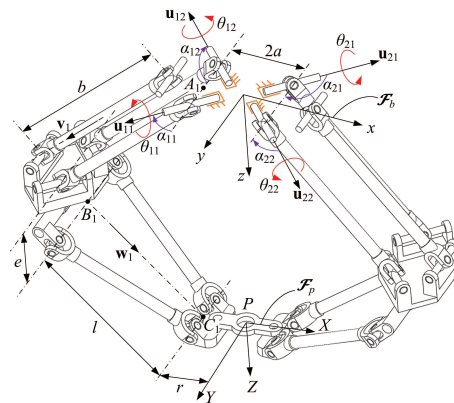


Figure 2. Kinematic structure of the two-limb parallel Schönflies-motion robot

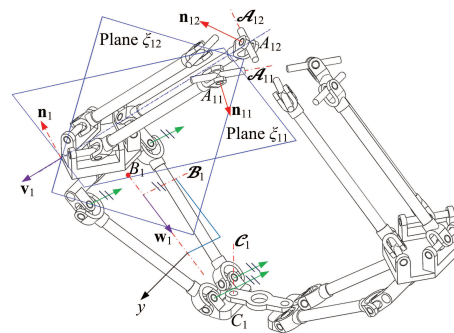


Figure 3. The loop structure of the robot with rotational inputs

2.3. Kinematic geometry of the manipulator

Under the coordinate systems of Figure 2, the position vectors of point A_i in frame \mathcal{F}_b are denoted by $\mathbf{a}_i = (-1)^i \mathbf{a}_i$, then the Cartesian coordinates of point B_i is derived as (3).

$$\mathbf{b}_i = b\mathbf{v}_i + \mathbf{a}_i; \quad \mathbf{v}_i = \mathbf{R}_i \mathbf{k} = \mathbf{R}_{i1} \mathbf{R}_{i2} \mathbf{k} \quad (3)$$

Where $\mathbf{R}_{ij} = \mathbf{R}(z, \alpha_{ij})\mathbf{R}(y, \theta_{ij})$ and θ_{ij} is the input angle from the reference plane.

Let the mobile platform pose be denoted by $\chi = [\mathbf{p}^T \ \phi]^T$, $\mathbf{p} = [x \ y \ z]^T$, the Cartesian coordinates of point C_i is expressed as (4).

$$\mathbf{c}_i = \mathbf{Q}\mathbf{c}'_i + \mathbf{p} \quad (4)$$

Where $\mathbf{Q} = \mathbf{R}(z, \phi)$ is the rotation matrix of the MP and $\mathbf{c}'_i = (-1)^i r \mathbf{i}$ is the position vector of point C_i in the frame \mathcal{F}_p .

2.3.1. Forward geometry

Due to translational motion of the distal spatial modules, the y -coordinate of point B_i is equal to that of C_i , thus, the y -coordinate of point P and the orientation of the mobile platform, respectively, are derived as (5).

$$y = \frac{1}{2} \sum_{i=1}^2 \mathbf{b}_i^T \mathbf{j}; \quad \phi = \sin^{-1} \frac{(\mathbf{b}_2 - \mathbf{b}_1) \mathbf{j}}{2r} \quad (5)$$

On the other hand, the x - and z -coordinates of point P of the mobile platform can be solved from the four-bar linkage as shown in Figure 4, namely, expressed as (6).

$$l(\sin q_1 - \sin q_2) + g_1 = 0; \quad l(\cos q_1 + \cos q_2) + g_2 = 0 \quad (6)$$

Where $g_1 = (\mathbf{b}_2 - \mathbf{b}_1)^T \mathbf{k}$ and $g_2 = 2r \cos \phi + (\mathbf{b}_1 - \mathbf{b}_2)^T \mathbf{i}$. Consequently, the angles $q_1, q_2 \in [0, \pi/2]$ are obtained as (7).

$$q_1 = 2 \tan^{-1} \frac{2g_1 \pm \sqrt{4g_1^2 + 4g_2^2 - (g_1^2 + g_2^2)^2}}{g_1^2 + g_2^2 - 2g_2}; \quad q_2 = \sin^{-1}(\sin q_1 + g_1) \quad (7)$$

To this end, one obtains the x - and z -coordinates of point P in the frame \mathcal{F}_b is expressed as (8).

$$x = \frac{1}{2} \sum_{i=1}^2 \mathbf{c}_i^T \mathbf{i}; \quad z = \frac{1}{2} \sum_{i=1}^2 \mathbf{c}_i^T \mathbf{k} \quad (8)$$

Where $\mathbf{c}_i = \mathbf{b}_i + l\mathbf{w}_i$, $\mathbf{w}_i = [(-1)^{i+1} \cos q_i \ 0 \ \sin q_i]^T$, stands for the position vector of point C_i .

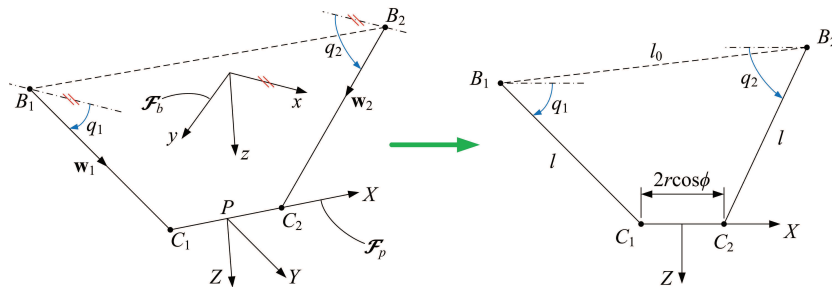


Figure 4. The planar four-bar linkage $B_1C_1C_2B_2$ in the forward geometry

2.3.2. Inverse geometry

The inverse geometric problem is solved from the following kinematic constraints expressed as (9) and (10).

$$(\mathbf{c}_i - \mathbf{b}_i) \cdot \mathbf{j} = 0, \quad i = 1, 2 \quad (9)$$

$$(\mathbf{c}_i - \mathbf{b}_i)^T (\mathbf{c}_i - \mathbf{b}_i) = l^2 \quad (10)$$

Expanding the above equations leads to (11a) and (11b).

$$D_{11}^i \sin \theta_{i1} + D_{12}^i \cos \theta_{i1} + d_1^i = 0 \quad (11a)$$

$$D_{21}^i \sin \theta_{i1} + D_{22}^i \cos \theta_{i1} + d_2^i = 0 \quad (11b)$$

Which can be cast in a matrix form as (12).

$$\begin{bmatrix} D_{11}^i & D_{12}^i \\ D_{21}^i & D_{22}^i \end{bmatrix} \begin{bmatrix} \sin \theta_{i1} \\ \cos \theta_{i1} \end{bmatrix} = \mathbf{D}_i \begin{bmatrix} \sin \theta_{i1} \\ \cos \theta_{i1} \end{bmatrix} = - \begin{bmatrix} d_1^i \\ d_2^i \end{bmatrix} \quad (12)$$

With the coefficients expressed as (13a), (13b), and (14a) to (14e).

$$D_{11}^i = h_{i1} c \theta_{i2}; \quad D_{12}^i = h_{i2} s \theta_{i2}; \quad D_{21}^i = h_{i3} s \theta_{i2} + h_{i4} c \theta_{i2}; \quad D_{22}^i = h_{i5} s \theta_{i2} + h_{i6} c \theta_{i2} \quad (13a)$$

$$d_1^i = d_{i1} s \theta_{i2} + d_{i2}; \quad d_2^i = d_{i3} s \theta_{i2} + d_{i4} \quad (13b)$$

$$h_{i1} = -b s \alpha_{i1}; \quad h_{i2} = -b c \alpha_{i2} s \alpha_{i1} \quad (14a)$$

$$h_{i3} = 2b z c \alpha_{i2}; \quad h_{i4} = -2b((x+a)c \alpha_{i1} + y s \alpha_{i1} - r c(\alpha_{i1} - \phi)) \quad (14b)$$

$$h_{i5} = -2b c \alpha_{i2}((x+a)c \alpha_{i1} + y s \alpha_{i1} - r c(\alpha_{i1} - \phi)); \quad h_{i6} = -2b z \quad (14c)$$

$$d_{i1} = -b c \alpha_{i1} s \alpha_{i2}; \quad d_{i2} = y - r s \phi \quad (14d)$$

$$d_{i3} = 2b s \alpha_{i2}((x+a)s \alpha_{i1} - y c \alpha_{i1} - r s(\alpha_{i1} - \phi)); \quad d_{i4} = \|\mathbf{c}_i - \mathbf{a}_i\|^2 + b^2 - l^2 \quad (14e)$$

Where s and c stand for the sine and cosine functions, respectively. The determinant of matrix \mathbf{D}_i is calculated as (15).

$$|\mathbf{D}_i| = 2b^2 z \sin \alpha_{i1} (1 - \sin^2 \alpha_{i2} \sin^2 \theta_{i2}) \neq 0 \quad (15)$$

Solving (12) using Cramer's rule, $\sin \theta_{i1}$ and $\cos \theta_{i1}$ can be obtained as the functions of θ_{i2} . Expanding and simplifying equation $\sin^2 \theta_{i1} + \cos^2 \theta_{i1} = 1$ yields expressed as (16) with (17a) to (17g).

$$S_1 \sin^4 \theta_{i2} + S_2 \sin^3 \theta_{i2} + S_3 \cos^2 \theta_{i2} \sin^2 \theta_{i2} + S_4 \sin^2 \theta_{i2} + S_5 \cos^2 \theta_{i2} \sin \theta_{i2} + S_6 \cos^4 \theta_{i2} + S_7 \cos^2 \theta_{i2} = 0 \quad (16)$$

$$S_1 = d_{i1}^2 (h_{i3}^2 + h_{i5}^2) - 2d_{i1}d_{i3}h_{i2}d_{i5} + h_{i2}^2 (d_{i3}^2 - h_{i3}^2) \quad (17a)$$

$$S_2 = 2d_{i1}d_{i2} (h_{i3}^2 + h_{i5}^2) + 2d_{i3}d_{i4}h_{i2}^2 - 2h_{i2}d_{i5} (d_{i1}d_{i4} + d_{i2}d_{i3}) \quad (17b)$$

$$S_3 = d_{i1}^2 (h_{i4}^2 + h_{i6}^2) - 2d_{i1}d_{i3}h_{i1}d_{i4} + h_{i1}^2 (d_{i3}^2 - h_{i5}^2) + 2h_{i1}h_{i2} (h_{i4}h_{i5} + h_{i3}h_{i6}) - h_{i2}^2 h_{i4}^2 \quad (17c)$$

$$S_4 = d_{i2}^2 (h_{i3}^2 + h_{i5}^2) - 2d_{i2}d_{i4}h_{i2}d_{i5} + h_{i2}^2 d_{i4}^2 \quad (17d)$$

$$S_5 = 2d_{i1}d_{i2} (h_{i4}^2 + h_{i6}^2) + 2d_{i3}d_{i4}h_{i1}^2 - 2h_{i1}d_{i4} (d_{i1}d_{i4} + d_{i2}d_{i3}) \quad (17e)$$

$$S_6 = -h_{i1}^2 h_{i6}^2 \quad (17f)$$

$$S_7 = d_{i2}^2 (h_{i4}^2 + h_{i6}^2) - 2d_{i2}d_{i4}h_{i1}d_{i4} + d_{i4}^2 h_{i1}^2 \quad (17g)$$

Equation (16) can be written in the following equivalent form (18) with (19).

$$\sin^4 \theta_{i2} + L_i \sin^3 \theta_{i2} + M_i \sin^2 \theta_{i2} + N_i \sin \theta_{i2} + P_i = 0 \quad (18)$$

$$L_i = \frac{S_2 - S_5}{S_1 - S_3 + S_6}; \quad M_i = \frac{S_3 + S_4 - 2S_6 - S_7}{S_1 - S_3 + S_6}; \quad N_i = \frac{S_5}{S_1 - S_3 + S_6}; \quad P_i = \frac{S_6 + S_7}{S_1 - S_3 + S_6} \quad (19)$$

As a result, angle θ_{i2} can be obtained by solving the Quartic (18), namely, expressed as (20) with (21), where expressed as (22a) to (22c).

$$\theta_{i2} = \sin^{-1} \left(-\frac{L_i}{4} - \frac{1}{2} \sqrt{\frac{L_i^2}{4} - \frac{2M_i}{3} + I_i + J_i} \pm \frac{1}{2} \sqrt{\frac{L_i^2}{2} - \frac{4M_i}{3} - I_i - J_i \pm K_i} \right) \quad (20)$$

$$I_i = \frac{\sqrt[3]{2}U_i}{3\sqrt[3]{W_i}}; \quad J_i = \sqrt[3]{\frac{W_i}{54}}; \quad K_i = \frac{1}{4} \frac{-L_i^3 + 4L_iM_i - 8N_i}{\sqrt{L_i^2/4 - 2M_i/3 + I_i + J_i}} \quad (21)$$

$$U_i = M_i^2 - 3L_iN_i + 12P_i \quad (22a)$$

$$V_i = 2M_i^3 - 9L_iM_iN_i + 27N_i^2 + 27L_i^2P_i - 72M_iP_i \quad (22b)$$

$$W_i = V_i + \sqrt{-4U_i^3 + V_i^2} \quad (22c)$$

Substituting θ_{i2} into (9), angle θ_{i1} is then solved as (23) with (24a) to (24c).

$$\theta_{i1} = 2 \tan^{-1} \frac{-X_i \pm \sqrt{X_i^2 + Y_i^2 - Z_i^2}}{Z_i - Y_i} \quad (23)$$

$$X_i = -b \sin \alpha_{i1} \cos \theta_{i2} \quad (24a)$$

$$Y_i = -b \cos \alpha_{i2} \sin \alpha_{i1} \sin \theta_{i2} \quad (24b)$$

$$Z_i = y - r \sin \phi - b \sin \alpha_{i2} \cos \alpha_{i1} \sin \theta_{i2} \quad (24c)$$

3. RESULTS AND DISCUSSION

3.1. Jacobian analysis

The Jacobian matrices of the robot can be obtained by differentiating (9) and (10) with respect to time. As the y -coordinate is independent of link length B_iC_i , here, in order to make these two equations homogeneously dimensionless, (9) and (10) can be rewritten as (25) and (26).

$$(\mathbf{c}_i - \mathbf{b}_i) \cdot \mathbf{j}/b = 0, \quad i = 1, 2 \quad (25)$$

$$(\mathbf{c}_i - \mathbf{b}_i)^T (\mathbf{c}_i - \mathbf{b}_i)/l^2 - 1 = 0 \quad (26)$$

Upon the differentiations of (25) and (26), one obtains expressed as (27) and (28).

$$(\dot{\phi} r \cos q_i \sin \phi + \mathbf{w}_i^T \dot{\mathbf{p}})/l = (\dot{\theta}_{i1} b \mathbf{w}_i^T (\mathbf{u}_{i1} \times \mathbf{v}_i) + \dot{\theta}_{i2} b \mathbf{w}_i^T (\mathbf{u}_{i2} \times \mathbf{v}_i))/l \quad (27)$$

$$((-1)^i \dot{\phi} r \cos \phi + \mathbf{j}^T \dot{\mathbf{p}})/b = \dot{\theta}_{i1} \mathbf{j}^T (\mathbf{u}_{i1} \times \mathbf{v}_i) + \dot{\theta}_{i2} \mathbf{j}^T (\mathbf{u}_{i2} \times \mathbf{v}_i) \quad (28)$$

Where $\dot{\mathbf{p}} = [\dot{x} \quad \dot{y} \quad \dot{z}]^T$. Equations (27) and (28) can be cast in a matrix form, namely, expressed as (29) with (30a) to (30c).

$$\mathbf{A} \dot{\chi} = \mathbf{B} \dot{\theta} \quad (29)$$

$$\mathbf{A} = \begin{bmatrix} \cos q_1 & 0 & \sin q_1 & r \cos q_1 \sin \phi \\ 0 & l/b & 0 & -rl/b \cos \phi \\ -\cos q_2 & 0 & \sin q_2 & r \cos q_2 \sin \phi \\ 0 & l/b & 0 & rl/b \cos \phi \end{bmatrix} \quad (30a)$$

$$\mathbf{B} = \begin{bmatrix} \mathbf{B}_1 & \mathbf{0}_2 \\ \mathbf{0}_2 & \mathbf{B}_2 \end{bmatrix} = \begin{bmatrix} b \mathbf{w}_1^T (\mathbf{u}_{11} \times \mathbf{v}_1) & b \mathbf{w}_1^T (\mathbf{u}_{12} \times \mathbf{v}_1) & 0 & 0 \\ l \mathbf{j}^T (\mathbf{u}_{11} \times \mathbf{v}_1) & l \mathbf{j}^T (\mathbf{u}_{12} \times \mathbf{v}_1) & 0 & 0 \\ 0 & 0 & b \mathbf{w}_2^T (\mathbf{u}_{21} \times \mathbf{v}_2) & b \mathbf{w}_2^T (\mathbf{u}_{22} \times \mathbf{v}_2) \\ 0 & 0 & l \mathbf{j}^T (\mathbf{u}_{21} \times \mathbf{v}_2) & l \mathbf{j}^T (\mathbf{u}_{22} \times \mathbf{v}_2) \end{bmatrix} \quad (30b)$$

$$\dot{\chi} = [\dot{x} \quad \dot{y} \quad \dot{z} \quad \dot{\phi}]^T; \quad \dot{\theta} = [\dot{\theta}_1 \quad \dot{\theta}_2 \quad \dot{\theta}_3 \quad \dot{\theta}_4]^T \quad (30c)$$

Where \mathbf{A} and \mathbf{B} are the forward and backward Jacobians, respectively. As long as \mathbf{A} is nonsingular, the kinematic Jacobian matrix is obtained as (31).

$$\mathbf{J} = \mathbf{A}^{-1} \mathbf{B} \quad (31)$$

3.1.1. Singularity analysis

The three types of singularities can be determined from the Jacobian matrices in (29) namely, i) $\det(\mathbf{B}) = 0$, the robot loses one or more DOF and reaches a serial singularity; ii) $\det(\mathbf{A}) = 0$, the robot gains one or more uncontrolled DOF and encounters a parallel singularity; and iii) $\det(\mathbf{A}) = \det(\mathbf{B}) = 0$, the robot is in a configuration of mixed singularity. Here, we only focus on the first two types of singularities, as this type of singularities can be obtained from the two previous ones.

From $\det(\mathbf{B}) = \det(\mathbf{B}_1) \cdot \det(\mathbf{B}_2)$, the robot reaches type 1 singularity in the configuration $\mathbf{u}_{ij} \parallel \mathbf{v}_i$ or/and $\mathbf{w}_i \parallel \mathbf{v}_i$, which usually occurs at the workspace boundaries. The type 2 singularities arise when $\mathbf{w}_1 \parallel \mathbf{w}_2$, i.e., $q_1 = q_2 = 0$ or $q_1 = q_2 = \pi/2$ or $\phi = \pm\pi/2$, which leads to the uncontrollable motion of the mobile platform.

3.1.2. Isotropic configuration

The manipulator isotropy is often related to the dexterity, and the Jacobian matrix is said to be isotropic under the conditions expressed as (32).

$$\mathbf{A}^T \mathbf{A} = \tau^2 \mathbf{I}_4; \quad \mathbf{B}^T \mathbf{B} = \sigma^2 \mathbf{I}_4 \quad (32)$$

Where τ and σ denote the four identical singular values that each Jacobian matrix must have at the optimum postures, and \mathbf{I} in the identity matrix. As the entries of the forward Jacobian matrix of the robot are not homogeneous as they contain mixed rotation and translation terms, for which the condition number is limited to indicate the kinematic performance. Here, the characteristic length is introduced to normalize the forward Jacobian matrix [21], where the characteristic length L_c is obtained as (33).

$$\mathbf{A} \dot{\chi} = [\mathbf{A}_v \quad \mathbf{A}_\omega] \begin{bmatrix} \dot{\mathbf{p}} \\ \dot{\phi} \end{bmatrix} = [\mathbf{A}_v \quad \mathbf{A}_\omega/L_c] \begin{bmatrix} \dot{\mathbf{p}} \\ L_c \dot{\phi} \end{bmatrix} = \bar{\mathbf{A}} \dot{\chi}' \quad (33)$$

Where \mathbf{A}_v is the first three columns and \mathbf{A}_ω is the last one in \mathbf{A} , respectively, and $\bar{\mathbf{A}}$ is the dimensional homogeneous Jacobian. Consequently, the isotropy condition can be expressed as (34).

$$\bar{\mathbf{A}}^T \bar{\mathbf{A}} = \begin{bmatrix} \mathbf{A}_v^T \mathbf{A}_v & \mathbf{A}_v^T \mathbf{A}_\omega/L_c \\ \mathbf{A}_\omega^T \mathbf{A}_v/L_c & \mathbf{A}_\omega^T \mathbf{A}_\omega/L_c^2 \end{bmatrix} = \begin{bmatrix} \tau^2 \mathbf{I}_3 & \mathbf{0} \\ \mathbf{0}^T & \tau^2 \end{bmatrix} \quad (34)$$

Hence, the characteristic length is obtained as (35).

$$L_c = \sqrt{\frac{3\mathbf{A}_\omega^T \mathbf{A}_\omega}{\text{tr}(\mathbf{A}_v^T \mathbf{A}_v)}} \quad (35)$$

Substituting (35) into (34) yields expressed as (36) with the characteristic length and the identical singular value, respectively, expressed as (37).

$$q_1 = q_2 = \pi/4 \quad (36)$$

$$L_c = r; \quad \tau = 1 \quad (37)$$

The backward Jacobian matrix \mathbf{B} is isotropic when $\mathbf{B}^T \mathbf{B} = \sigma^2 \mathbf{I}_4$, consequently, the common singular value is found as (38) with the isotropic configurations as (39).

$$\begin{cases} \sigma = 1; & \theta_{ij} = 0 \\ \sigma = 1/\sqrt{5}; & \theta_{i1} = 0, -\theta_{12} = \theta_{22} = \tan^{-1} 2 \end{cases} \quad (38)$$

$$\begin{cases} x = 0, y = 0, z = b + l/\sqrt{2}, \phi = 0; & \sigma = 1 \\ x = 0, y = 0, z = b/\sqrt{5} + l/\sqrt{2}, \phi = 0; & \sigma = 1/\sqrt{5} \end{cases} \quad (39)$$

In accordance with (39), it is seen that the isotropic configurations are related to both manipulator pose and the geometric parameters. For the robot under study, its isotropic configurations exist when the design parameters meet the following conditions as (40).

$$l = \sqrt{2}(a - r), b = \sqrt{2}l \quad \text{or} \quad l = \sqrt{2}(a - r - b/\sqrt{5}), b = \sqrt{2}l \quad (40)$$

In practice, the first case, i.e., $l = \sqrt{2}(a - r)$, $b = \sqrt{2}l$, can be selected as the design candidate to define the home configuration of the robot because of $\theta_{ij} = 0$, which is in an isotropic configuration.

4. CONCLUSION

In this paper, a new two-limb parallel Schönflies-motion generator is introduced, which adopts a pair of alternative spatial module equivalent to the parallelogram structure. Compared to the fully symmetrical four-limb counterparts, this robot architecture can help to save the shop-floor space, allowing more robots to be deployed in the production line side-by-side, to improve the productivity. Moreover, this modular architecture can ensure the enhanced stiffness of the manipulator normal to the motion of the planar parallelogram structure.

The mobility of the robot is verified with the Lie group, which shows that the robot can generate Schönflies-motion. Similar to other types of two-limb SMGs, the forward geometry problem of the new configuration is simple, and the inverse geometric problem can also be solved symbolically. The manipulator singularity is studied by means of the Jacobian method, where singular configurations are identified. Moreover, the kinematic isotropy is investigated in pursuit of the identical singular values of the homogenous Jacobian matrices. An isotropic configuration of the robot, which can be considered as the neutral configuration, is detected, showing the geometric relationship of the link lengths for the robot structural design. The mechanical design of the robot prototype is under way for experimental validation and testing. Future work will focus on the robot dynamics and control.

ACKNOWLEDGEMENT

The support from Fundamental Research Funds for the Central Universities (No. DUT19JC25) are gratefully acknowledged.





REFERENCES

- [1] S. Krut, V. Nabat, O. Company, and F. Pierrot, "A high-speed parallel robot for Scara motions," *IEEE International Conference on Robotics and Automation, 2004. Proceedings. ICRA '04. 2004*, 2004, pp. 4109-4115 Vol.4, doi: 10.1109/ROBOT.2004.1308914.
- [2] F. Pierrot, V. Nabat, O. Company, S. Krut, and P. Poignet, "Optimal design of a 4-DOF parallel manipulator: from academia to industry," in *IEEE Transactions on Robotics*, vol. 25, no. 2, pp. 213-224, April 2009, doi: 10.1109/TRO.2008.2011412.
- [3] S. M. Kim, W. Kim, and B. Yi, "Kinematic analysis and optimal design of a 3T1R type parallel mechanism," *2009 IEEE International Conference on Robotics and Automation*, 2009, pp. 2199-2204, doi: 10.1109/ROBOT.2009.5152771.
- [4] O. Altuzarra, B. S. andru, C. Pinto, and V. Petuya, "A symmetric parallel Schonflies-motion manipulator for pick-and-place operations," *Robotica*, vol. 29, pp. 853-862, 2011, doi: 10.1017/S0263574711000063.
- [5] S. Liu, T. Huang, J. Mei, X. Zhao, P. Wang, and D. G. Chetwynd, "Optimal design of a 4-DOF SCARA type parallel robot using dynamic performance indices and angular constraints," *ASME Journal of Mechanical Robotics*, vol. 4, no. 3, p. 031005, 2012, doi: 10.1115/1.4006743.
- [6] F. Xie and X. Liu, "Design and development of a high-speed and high-rotation robot with four identical arms and a single platform," *ASME Journal of Mechanical Robotics*, vol. 7, no. 4, p. 041015, 2015, doi: 10.1115/1.4029440.
- [7] G. Wu, S. Bai, and P. Hjørnet, "On the stiffness of three/four degree-of-freedom parallel pick-and-place robots with four identical limbs," *2016 IEEE International Conference on Robotics and Automation (ICRA)*, 2016, pp. 861-866, doi: 10.1109/ICRA.2016.7487217.
- [8] T. Yang, A. Liu, H. Shen, and L. Hang, "Topological structure synthesis of 3t1r parallel mechanism based on poc equations," in *International Conference on Intelligent Robotics and Applications*, 2016, pp. 147-161, doi: 10.1007/978-3-319-43506-0_13.
- [9] G. Wu, S. Bai, and P. Hjørnet, "Architecture optimization of a parallel Schonflies-motion robot for pick- and-place applications in a predefined workspace," *Mechanism and Machine Theory*, vol. 106, pp. 148-165, 2016, doi: http: 10.1016/j.mechmachtheory.2016.09.005.
- [10] J. Angeles, S. Caro, W. A. Khan, and A. Morozov, "Kinetostatic design of an innovative Schonflies-motion generator," *ARCHIVE Proceedings of the Institution of Mechanical Engineers Part C Journal of Mechanical Engineering Science 1989-1996*, 2006, vol. 220, no. 7, pp. 935-943, doi: 10.1243/09544062JMES258.
- [11] P. C. Lee and J. J. Lee, "Singularity and workspace analysis of three isoconstrained parallel manipulators with schoenflies motion," *Frontiers of Mechanical Engineering*, vol. 7, pp. 163-187, 2012, doi: 10.1007/s11465-012-0324-5.
- [12] T. Harada and J. Angeles, "Kinematics and singularity analysis of a CRRHRRRC parallel Schonflies motion generator," *Transactions-Canadian Society for Mechanical Engineering*, vol. 38, no. 2, pp. 173-183, 2014, doi: 10.1139/tcsme-2014-0012.
- [13] L. Xu, Q. Chen, L. He, and Q. Li, "Kinematic analysis and design of a novel 3T1R 2-(PRR)2RH hybrid manipulator," *Mechanism and Machine Theory*, vol. 112, pp. 105-122, 2017, doi: 10.1016/j.mechmachtheory.2017.01.009.
- [14] R. Di Gregorio and H. Simas, "Dimensional synthesis of the single-loop translational parallel manipulator PRRR-PRPU," *Meccanica*, vol. 53, no. 1, pp. 481-495, 2018, doi: 10.1007/s11012-017-0702-5.
- [15] P. K. Eskandary and J. Angeles, "The dynamics of a parallel Schoenflies-motion generator," *Mechanism and Machine Theory*, vol. 119, pp. 119-129, 2018, doi: 10.1016/j.mechmachtheory.2017.09.006.
- [16] S. M. Kim, K. Shin, B.-J. Yi, and W. Kim, "Development of a novel two-limbed parallel mechanism having schonflies motion," *Proceedings of the Institution of Mechanical Engineers, Part C: Journal of Mechanical Engineering Science*, 2014, vol. 229, no. 1, pp. 136-154, doi: 10.1177/0954406214532633.
- [17] C. Wu, G. Yang, C. -Y. Chen, S. Liu, and T. Zheng, "Kinematic design of a novel 4-DOF parallel manipulator," *2017 IEEE International Conference on Robotics and Automation (ICRA)*, 2017, pp. 6099-6104, doi: 10.1109/ICRA.2017.7989724.





- [18] G. Wu and Z. Ping, "Stiffness analysis and comparison of a biglide parallel grinder with alternative spatial modular parallelograms," *Robotica*, vol. 35, no. 6, pp. 1310–1326, 2017, doi: 10.1017/S0263574716000059.
- [19] C. Germain, S. Caro, S. Briot, and P. Wenger, "Singularity-free design of the translational parallel manipulator IRSBot-2," *Mechanism and Machine Theory*, vol. 64, no. 6, pp. 262–285, 2013, doi: 10.1016/j.mechmachtheory.2013.02.005.
- [20] G. Wu, "Optimal structural design of a biglide parallel drill grinder," *The International Journal of Advanced Manufacturing Technology*, vol. 90, no. 9, pp. 2979–2990, 2017, doi: 10.1007/s00170-016-9625-x.
- [21] J. Angeles, "Is there a characteristic length of a rigid-body displacement?" *Mechanism and Machine Theory*, vol. 41, no. 8, pp. 884–896, 2006, doi: 10.1016/j.mechmachtheory.2006.03.010.

BIOGRAPHIES OF AUTHORS



Guanglei Wu     is an associate professor at School of Mechanical Engineering in Dalian University of Technology since July 2016. He received his PhD in Mechanical Engineering from Aalborg University (2013), Denmark, and MSc in Mechanical Design and Manufacture from Northeastern University (2009), Shenyang, China. He was granted an industrial project by Innovation Fund Denmark and worked as a postdoc fellow in Aalborg University from 2014 to 2016. He was a visiting scholar in the Research Institute in Communications and Cybernetics of Nantes (IRCCyN, the former LS2N) in 2012. His research interests include conceptual design of robots, performance evaluation of parallel mechanisms, design optimization and industrial robots. Particularly, he specializes in robotic technologies including robot design and their industrial applications. His research work related to those fields has been published in *Mechanism and Machine Theory*, *ASME Journal of Mechanical Design*, *ASME Journal of Mechanisms and Robotics*, *IEEE ICRA*, and *IROS* conferences, and has been internationally recognized. He is the referee of a number of international journals and conferences in the fields of mechanisms and robots. He can be contacted at email: gwu@dlut.edu.cn.



Huiping Shen     is professor and a doctoral tutor. He received the Bachelor degree in Jiangxi University of Science and Technology in 1984, the Master degree in Southeast University in 1989 and the Doctoral degree in Jiangsu University in 2006, respectively. He has been working for Changzhou University since 1989, and was appointed as associate professor, professor and doctoral tutor in 1995, 2001, and 2010 respectively. He was awarded Special Allowance from the central government of P. R. China as an Excellent Expert in 2001. He completed sixteen projects founded by Natural Science Foundation of Jiangsu province and 35 projects supported by companies in P. R. China. Dr. Shen and his team members published about 260 research papers and he holds 70 patents of novel robot mechanisms. He can be contacted at email: shp65@126.com.
Scholar, Scopus, Publons and ORCID: unavailable.